

## THE DISSOCIATIVE ELECTROIONIZATION OF AMMONIA AND AMMONIA- $d_3$ . II. THE $H^+$ AND $H_2^+$ DISSOCIATION CHANNELS

R. LOCHT, Ch. SERVAIS, M. LIGOT, M. DAVISTER and J. MOMIGNY

*Département de Chimie Générale et de Chimie Physique, Institut de Chimie, Bâtiment B6, Université de Liège, Sart-Tilman par B-4000 Liège 1, Belgium*

### Abstract

The dissociative electroionization of  $NH_3$  ( $ND_3$ ), in the  $H^+$  ( $D^+$ ) and  $H_2^+$  ( $D_2^+$ ) dissociation channels, is investigated in the 18-50 eV electron energy range. The  $H^+$  ( $D^+$ ) translational energy distribution spectrum shows several components and that of  $H_2^+$  ( $D_2^+$ ) is continuous. The thermal energy component of the latter distribution is entirely ascribed to  $H_2^+$ / $H_2$ . For both ions the kinetic energy versus appearance energy diagram is obtained and discussed. The  $H^+$  ion at the lowest onset is probably formed at the expense of  $NH_3^+$  ( $\tilde{A}^2E$ ) state. In the 22.5 eV electron energy range both  $H^+$  and  $H_2^+$  are formed by dissociative autoionization. Evidence is also brought for  $H^+$  and  $H_2^+$  formation at 22.5 and 26.5 eV through spontaneous decomposition of  $NH_2^+$ . Above 35 eV dissociation of doubly ionized states by Coulomb repulsion is mainly involved.

### 1. Introduction

Recently, the results on the dissociative ionization of  $NH_3$  in the  $NH_2^+$  and  $NH^+$  dissociation channels have been reported [1]. Translational energy distribution measurements, together with appearance energy determinations allowed us to discuss in detail most of the dissociation processes.

The dissociation of  $NH_3$  into  $H^+$  and  $H_2^+$  has been investigated by a few groups. Appearance energies were measured but very briefly discussed without kinetic energy measurements. The earliest work of Mann et al. [2] and the most recent publication of Mark et al. [3] included both ions. Only the former discussed dissociation processes, while the latter only mentioned onset energies.

Using energy-loss electron spectroscopy and electron-ion coincidence technique, Wight et al. [4] and Brion et al. [5] determined the fragmentation pattern of  $NH_3$ , including the  $H^+$  dissociation channels.

More recently Carnahan et al. [6] and Kurawaki and Ogawa [7] published their results on high Rydberg H atoms and excited H ( $n=2, 3, 4$ ) atoms produced by electron impact on  $NH_3$ . Time-of-flight distribution and Doppler profile analysis of Balmer emission lines were used to derive kinetic energy distributions. Dissociative excitation processes, discussed in detail by the authors, can be linked to dissociative ionization work through the "core-ion" model [8,9].

This paper deals with the dissociative electroionization of  $NH_3$  in the  $H^+$  and  $H_2^+$  dissociation channels, including detailed ion translational energy analysis. The results on  $D^+$  and  $D_2^+$  from  $ND_3$  have been added. The 15-50 eV electron energy range is covered in order to include the  $NH_3$  double ionization energy range. Preliminary results on this particular aspect have already been published earlier [1,10].

### 2. Experimental

The experimental technique, as well as its most recent modifications used in the present work, have extensively been described elsewhere [11,12]. Briefly, the ions produced in a Nier-type ion source by the impact of energy-controlled electrons are allowed to drift out of the ion chamber, are focused on the ion source exit hole, energy analyzed by a retarding lens and mass selected in a quadrupole filter. The detected ion current is continuously scanned as a function of either the electron energy at fixed retarding potential  $V_R$  or the retarding potential at fixed electron energy  $E_e$ . Both signals are electronically differentiated. The experiment is almost computer controlled.

The experimental conditions are identical with those described previously [1]. Ammonia (Air Liquide, 99.95%) and ammonia- $d_3$  (Merk, Sharp & Dome 99.7%) samples, distilled under vacuum, are introduced at  $10^{-7}$  Torr as measured in the vacuum chamber.

The maximum of the  $\text{NH}_3^+$  ( $\text{ND}_3^+$ ) ion energy distribution is used as zero-energy calibration point of the translational energy scale. The appearance energy of  $\text{NH}_2^+$  ( $\text{ND}_2^+$ ), i.e.  $15.72 \pm 0.1$  eV is used to calibrate the electron energy scale.

For each fragment ion, at each retarding potential or electron energy setting, the first derivative of the ionization efficiency curve or of the retarding potential curve is scanned 100-800 times. This procedure is repeated at least five times. The energies quoted in the next sections are average values of these five independent measurements. The quoted errors and drawn error bars are given by the standard deviation. In the diagrams, linear regressions are fitted to the experimental data.

### 3. Experimental results

As an introductory remark, it has to be pointed out that beside  $\text{NH}_3$ , two different proton sources could be suspected, (i) Notwithstanding its low intensity after prolonged back out,  $\text{H}_2\text{O}$  is present in the background mass spectrum and produces  $\text{H}^+$  with a large cross section. (ii) As will be shown below  $\text{H}_2^+$  is probably formed through ionization of  $\text{H}_2$  produced by pyrolysis of  $\text{NH}_3$  on the electron emitting filament. Furthermore  $\text{H}_2^+$  is observed in the  $\text{H}_2\text{O}$  mass spectrum, though with very low intensity.

The simultaneous analysis of  $\text{D}^+/\text{ND}_3$  and  $\text{H}^+/\text{NH}_3$  would remove, at least to a large extent, the former proton source. On the other hand, the kinetic energy distribution and the appearance energies of  $\text{H}^+/\text{H}_2$  are available [13] and have to be kept in mind for the interpretation of the experimental results.

The same comments hold for  $\text{H}_2^+/\text{NH}_3$ . However, most confusing will be the thermal or nearly thermal  $\text{H}_2^+$  ( $\text{D}_2^+$ ) ions.

#### 3.1. The $\text{H}^+$ ( $\text{D}^+$ ) dissociation channel

Typical first differential retarding potential curves of  $\text{H}^+/\text{NH}_3$  and  $\text{D}^+/\text{ND}_3$ , as observed at 61 eV electron energy, are displayed in fig. 1. The identical shape of these curves indicates the absence of any contaminant, at least at low energy. Beside, a dominant low-energy peak, a shoulder at about 0.25 eV, slope changes around 0.6 eV and 1.5 eV, and finally a maximum near 4.0 eV are observed for  $\text{H}^+$ . These values slightly shift toward lower energies for  $\text{D}^+$ . The translational energy spectrum spreads up to 9 eV. Figs. 2 and 3 show the same distribution for  $\text{D}^+$  from 76-31 eV and 26.5-20.1 eV respectively. The maximum of the  $\text{ND}_3^+$  thermal ion energy distribution (see fig. 3) and the  $\text{D}^+$  low-energy peak only coincide for electron energies close to the lowest onset up to 23 eV. In the electron energy range 23-60 eV the same maximum regularly shifts upward to 45 meV. The same phenomenon is observed for  $\text{H}^+$  and is represented by the diagram in fig. 4. This means that the thermal  $\text{H}^+$  ions are only formed near the lowest onset. Above 23 eV only energetic protons are produced and dominate the translational energy spectrum.

At this point a comparison has to be made between the present results and those obtained for high Rydberg  $\text{H}(\text{Rydb.})$  atoms and excited  $\text{H}^*(n)$  atoms [6,7]. Concerning the position of the abovementioned features, the present  $\text{H}^+$  and  $\text{D}^+$  translational energy spectra agree fairly well with the  $\text{H}^*(n=2)$  [6]  $\text{H}^*(n=3,4)$  [7] kinetic energy spectra. However, the relative intensities are quite different, e.g. the distribution peaking at 4.0 eV dominates the  $\text{H}^*$  kinetic energy spectrum at 70 eV electron energy. Surprisingly even less agreement is found with the translational energy spectrum of  $\text{H}(\text{Rydb.})$  atoms [6], where a maximum at about 5.5 eV is the most intense feature. This could mean that at least for a number of processes leading to  $\text{H}(\text{Rydb.})$ , the "core-ion" model no longer holds.

The first differentiated ionization efficiency curves of  $\text{H}^+/\text{NH}_3$ , as observed for different retarding potential settings  $V_R$ , are shown in fig. 5. Vertical bars locate the average position of the successive appearance energies. The same measurements have been performed on  $\text{D}^+/\text{ND}_3$ . For comparison fig. 6 clearly shows both ions having almost the same first differentiated ionization efficiency curve. Six appearance energies have been measured, i.e.  $19.5 \pm 0.2$ ,  $22.6 \pm 0.3$ ,  $26.2 \pm 0.1$ ,  $34.9 \pm 0.4$ ,  $36.2 \pm 0.3$  and  $39.2 \pm 0.2$  eV. A critical energy is also measured at  $45.7 \pm 0.3$  eV and could only be observed for  $0.0 < V_R < 0.9$  V.

The kinetic energy versus appearance energy plot resulting from these measurements is displayed in fig. 7. The same plot for  $D^+/ND_3$ , restricted to the low energy range, is reproduced in fig. 8 together with the results on  $H^+/NH_3$  for comparison. Though both diagrams almost coincide within experimental error, systematic differences are observed which probably should be ascribed to isotope effects.

**Fig. 1.** The kinetic energy distribution curves of  $H^+/NH_3$  and  $D^+/ND_3$  observed at 61 eV electron energy.

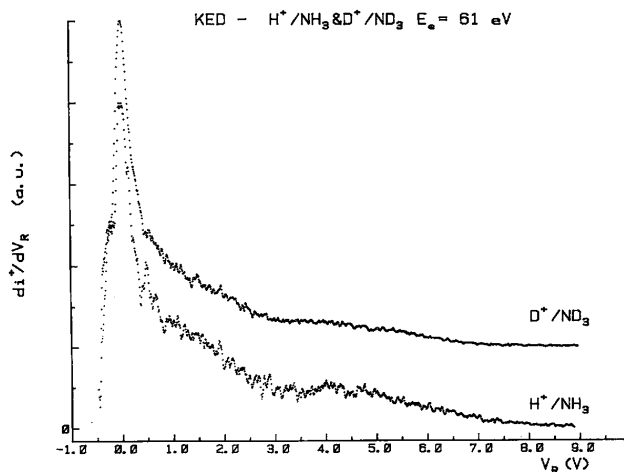


**Fig. 2.** Kinetic energy distribution spectra of  $D^+/ND_3$  recorded between 76 and 31 eV electron energy.

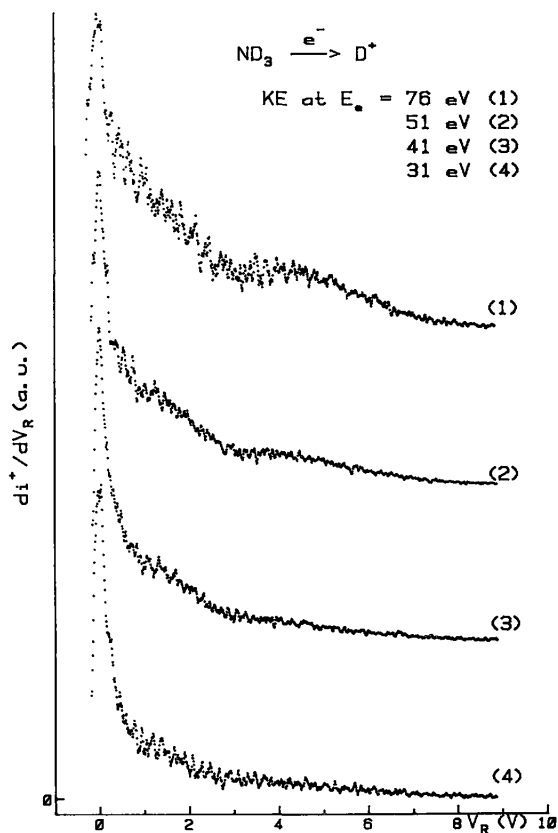


**Fig. 3.** Kinetic energy distribution spectra of  $D^+/ND_3$  recorded between 26.5 and 20.1 eV electron energy. The  $ND_3^+$  distribution is included for comparison.

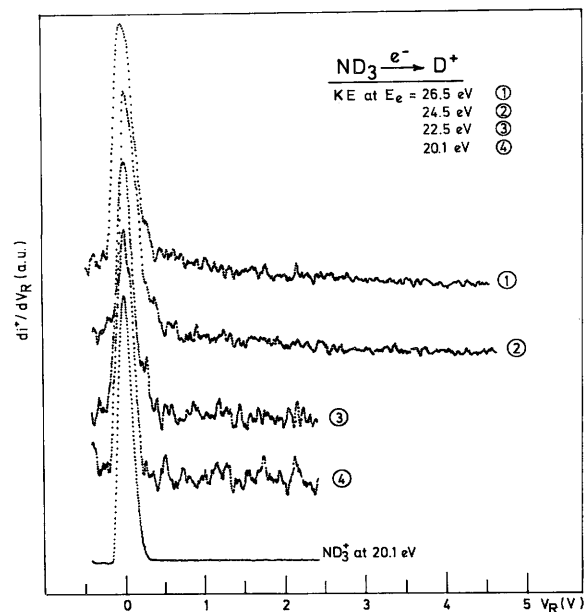
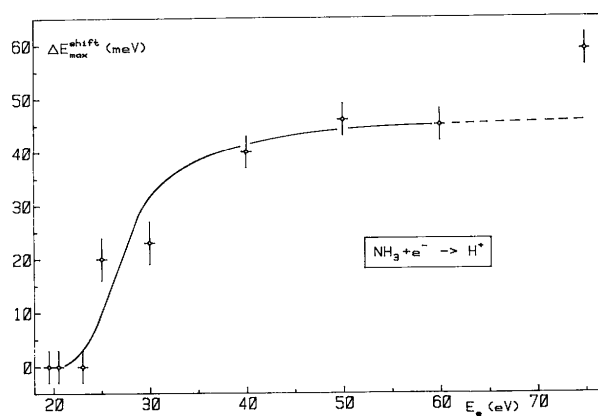


**Fig. 4.** Electron energy dependence of the position of the maximum of the  $H^+$  low-energy peak.



### 3.2. The $H_2^+$ ( $D_2^+$ ) dissociation channel

Despite its low intensity (about 0.05% of total ionization), the  $H_2^+$  ion has been investigated because of its potential importance for the interpretation of  $NH^+$  and  $N^+$  formation at high energies.

The  $D_2^+/ND_3$  translational energy distribution spectrum, as obtained by the first derivative of the retarding potential curve, is shown in fig. 9 for different impact energies of the electrons. The  $H_2^+/NH_3$  ion energy distribution is strictly identical. Both distributions exhibit an intense thermal energy peak and a long and structureless tail, extending to about 5 eV, which disappears below 26 eV electron energy.

The first differentiated ionization efficiency curves of  $D_2^+/ND_3$ , as observed for different values of the retarding potential, are displayed in fig. 10. In fig. 11 the same curve for  $H_2^+/NH_3$  is shown for comparison. For both ions, different appearance energies, marked by a vertical bar, are measured respectively at  $15.5 \pm 0.2$ ,  $22.3 \pm 0.2$ ,  $26.6 \pm 0.3$  and  $35.7 \pm 0.4$  eV. The kinetic energy versus appearance energy diagram for both  $H_2^+/NH_3$  and  $D_2^+/ND_3$  is represented in fig. 12.

**Fig. 5.** First differentiated ionization efficiency curves of  $H^+/NH_3$  as observed for indicated retarding potential ( $V_R$ ) settings. Vertical bars locate the average appearance energies.

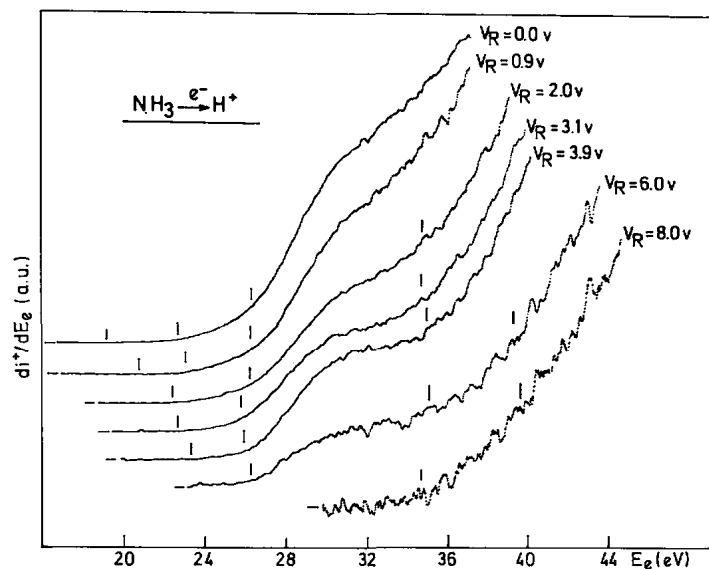
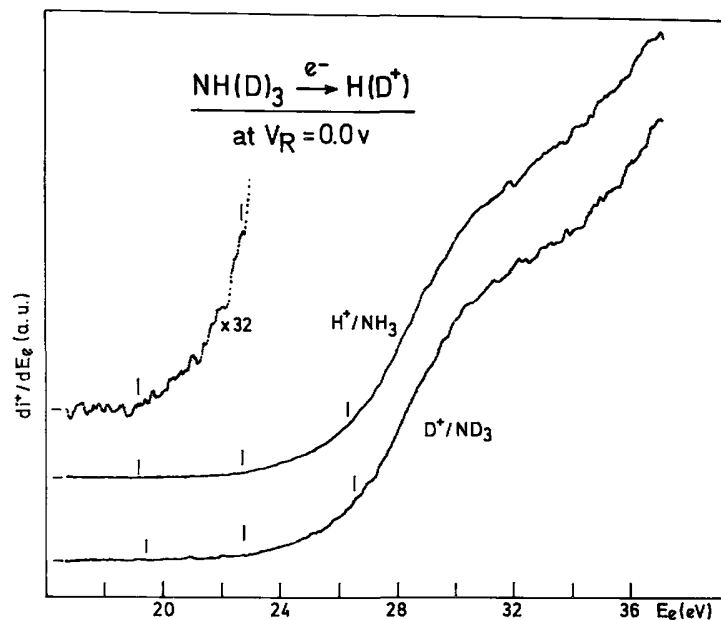


**Fig. 6.** Comparison of the first differentiated ionization efficiency curves of  $H^+/NH_3$  and  $D^+/ND_3$ , both recorded at  $V_R=0.0$  V. Vertical bars locate the average appearance energies at low electron energies.



#### 4. Discussion

For clarity in the following discussion, the results obtained in the present work are summarized in table 1. All the thermodynamical and spectroscopic data used to calculate critical energies are gathered in table 2.

##### 4.1. The $H^+$ ( $D^+$ ) dissociation channel

The lowest onset determined for the  $H^+$  production from  $NH_3^+$  is  $19.5 \pm 0.2$  eV. This result disagrees

drastically with previously published electron impact results, i.e.  $23.3 \pm 0.5$  eV [2] and  $23.0 \pm 0.2$  eV [3]. The discrepancy is at least of 3.5 eV. However, the present result is consistent with the measurements for  $D^+/ND_3$  for which an appearance energy of  $19.4 \pm 0.2$  is obtained (see fig. 8).

**Fig. 7.** The kinetic energy versus appearance energy plot for  $H^+/NH_3$ .

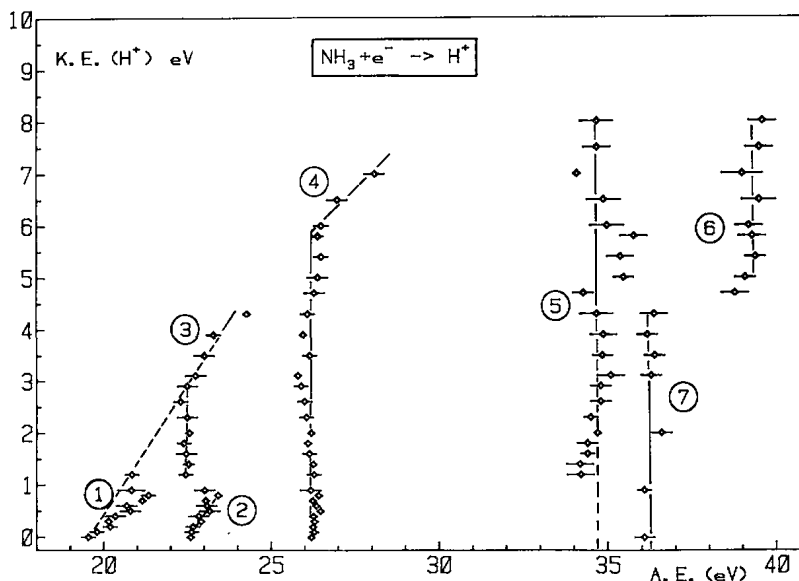
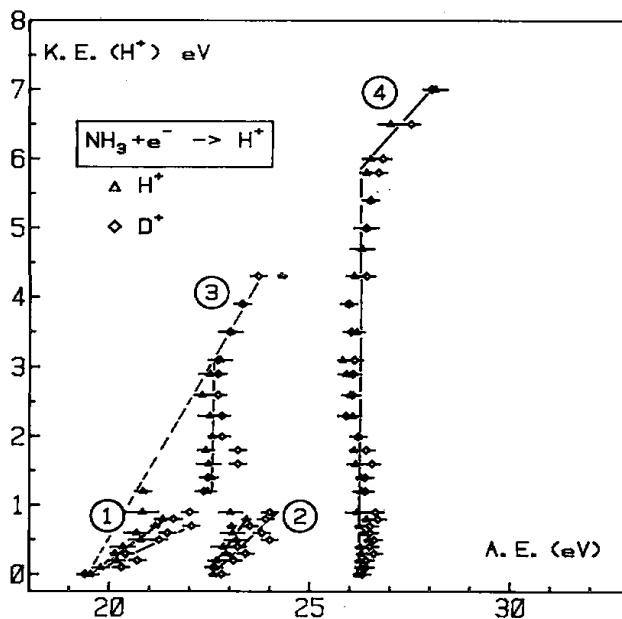


**Fig. 8.** The kinetic energy versus appearance energy plot for  $H^+/NH_3$  ( $\Delta$ ) and  $D^+/ND_3$  ( $\diamond$ ) between 18 and 33 eV electron energy.



The kinetic energy versus appearance energy diagram related to this threshold is the straight line (1) in fig. 7. In spite of the scattering of the onset measurements for 0-0.9 V retarding potential, a least-squares fit gives a correlation coefficient of 0.96 for a straight line extrapolating to 19.67 eV with a slope of 0.49. For the same measurements in  $D^+/ND_3$ , the straight line extrapolates to 19.62 eV with a slope of 0.29 and a correlation coefficient of 0.95.

**Fig. 9.** Kinetic energy distribution spectra of  $D_2^+/ND_3$  as observed at indicated electron energies.

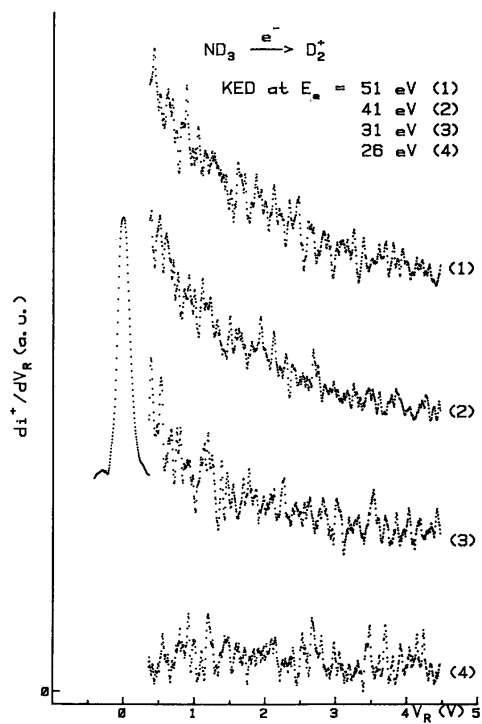


**Fig. 10.** First differentiated ionization efficiency curves of  $D_2^+/ND_3$  recorded at indicated retarding potential settings  $V_R$ . Vertical bars locate the average appearance energies.

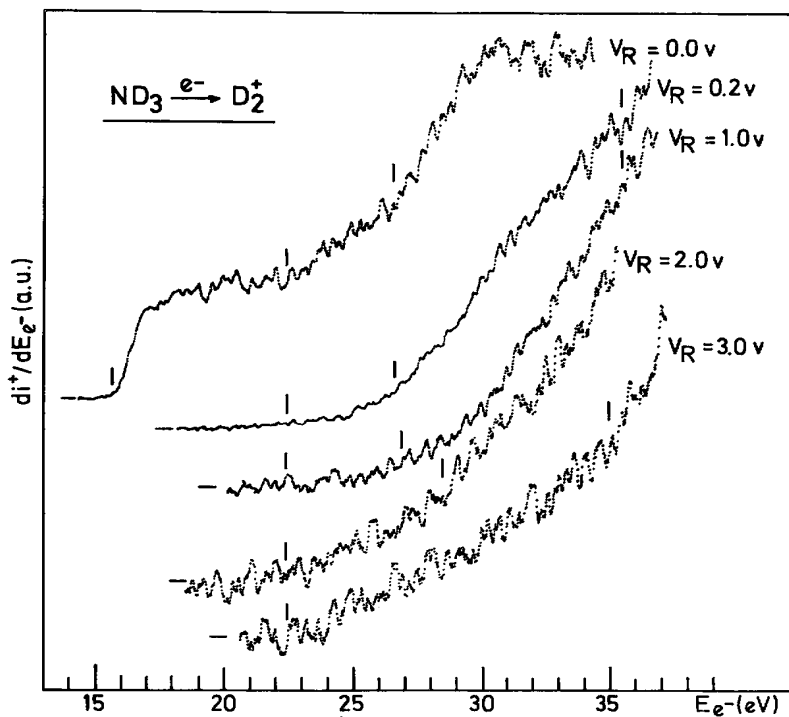


**Fig. 11.** First differentiated ionization efficiency curves of  $H_2^+/NH_3$  recorded at  $V_R=0.0$  V and 0.2 V shown for comparison with  $D_2^+/ND_3$ .

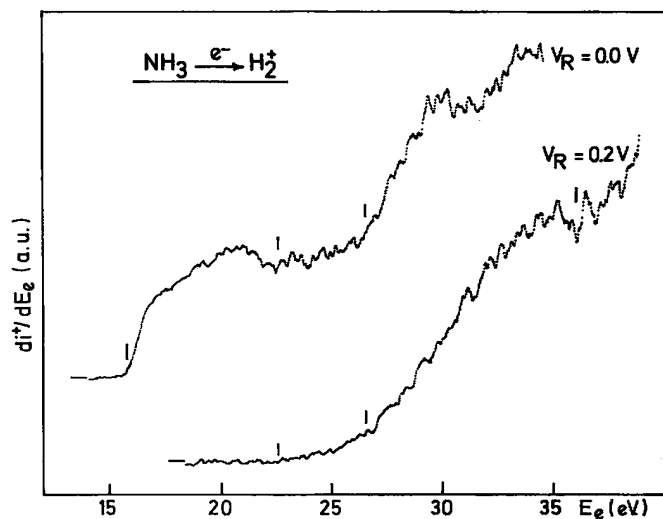


**Table 1.** The kinetic energy distributions (KED) and appearance energies (AE) (eV) for  $H^+$  ( $D^+$ ) and  $H_2^+$  ( $D_2^+$ ) from  $NH_3$  and  $ND_3$  as obtained in this work

	KED	AE
$H^+$ ( $D^+$ )	0.0-45 meV	$19.5 \pm 0.2$
	shift	$22.6 \pm 0.3$
	$\approx 0.25$	$26.2 \pm 0.1$
	$\approx 0.6$	$34.9 \pm 0.4$
	$\approx 1.5$	$36.2 \pm 0.3$
	$\approx 4.0$	$39.2 \pm 0.2$
$H_2^+$ ( $D_2^+$ )		$45.7 \pm 0.4$
	(0.0) <sup>a)</sup>	$(15.5 \pm 0.2)^{a)}$
		$22.3 \pm 0.2$
		$26.6 \pm 0.3$
		$35.7 \pm 0.4$

<sup>a)</sup> In parentheses data ascribed to  $H_2^+$  ( $D_2^+$ ) from  $H_2$  ( $D_2$ ).

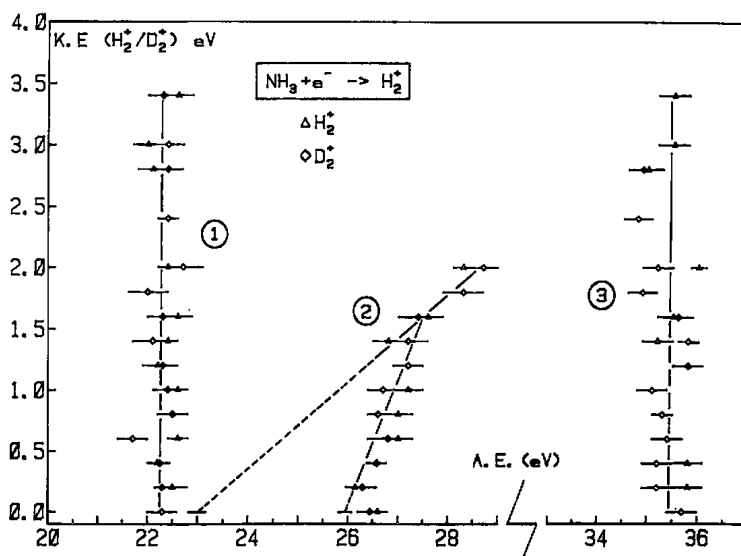
**Table 2.** Disociation energies ( $D$ ), ionization energies ( $IE$ ) and excitation energies ( $EE$ ) (eV) used in this work<sup>a)</sup>

$D(NH_2-H) = 4.51 \pm 0.09^b)$	$EE(NH_2^+(\tilde{X}^3B_1)) = 0.0^d)$
$D(NH-H) = 3.90 \pm 0.09^b)$	$EE(NH_2^+(\tilde{a}^1A_1)) = 0.99^d)$
$D(N-H) = 3.69^c)$	$EE(NH_2^+(\tilde{b}^1B_1)) = 2.23^d)$
$D(H-H) = 4.476^c)$	$EE(NH_2(\tilde{X}^2B_1)) = 0.0^f)$
	$EE(NH_2(\tilde{A}^2A_1)) = 1.27^f)$
$IE(NH_2) = 11.46 \pm 0.01^d)$	$EE(NH(X^3\Sigma^-)) = 0.0^g)$
$IE(NH) = 13.49 \pm 0.01^d)$	$EE(NH(a^1\Delta)) = 1.558^g)$
$IE(H_2) = 15.496^c)$	$EE(NH(b^1\Sigma^+)) = 2.629^g)$
$IE(H) = 13.595^c)$	$EE(NH(A^3\Pi)) = 3.69^g)$
$IE(N) = 14.549^c)$	$EE(NH(c^1\Pi)) = 5.423^g)$
	$EE(NH^+(X^2\Pi)) = 0.0^h)$
$EE(N(^4S)) = 0.0^e)$	$EE(NH^+(a^4\Sigma^-)) = 0.044^h)$
$EE(N(^2D)) = 2.38^e)$	$EE(NH^+(A^2\Sigma^-)) = 2.674^h)$
	$EE(NH^+(B^2\Delta)) = 2.847^h)$
	$EE(NH^+(C^2\Sigma^+)) = 4.409^h)$

<sup>a)</sup> 1 eV = 23.060 kcal mol<sup>-1</sup> = 8065.73 cm<sup>-1</sup>. <sup>b)</sup> Ref. [14]. <sup>c)</sup> Ref. [15]. <sup>d)</sup> Ref. [16]. <sup>e)</sup> Ref. [17]. <sup>f)</sup> Ref. [18]. <sup>g)</sup> Ref. [19]. <sup>h)</sup> Ref. [20].

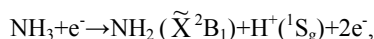


**Fig. 12.** The kinetic energy versus appearance energy plot for  $H_2^+/NH_3$  ( $\Delta$ ) and  $D_2^+/ND_3$  ( $\diamond$ ) between 20 and 36 eV electron energy.

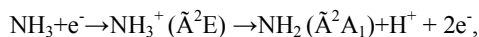


The slope of 0.49 could suggest that the observed  $H^+$  would be produced by dissociative ionization of  $H_2$ . As will be mentioned below,  $H_2$  is in fact produced very likely by thermolysis of  $NH_3$  on the electron emitting filament. In this case the linear dependence of the kinetic energy upon the electron energy would indeed be a straight line with a slope of 0.5. However, the same phenomenon being observed for  $ND_3$ , the same slope of 0.5 has to be expected. Experimentally a slope of 0.29 is observed. Furthermore, the appearance energy of  $H^+/H_2$  is well below 19.5 eV, i.e. 18.1 eV [13].

The lowest energy required for the production of  $H^+$  from  $NH_3$  through



is calculated at 18.105 eV, based on the data listed in table 2. As shown in fig. 6, in the first differentiated ionization efficiency curve of  $H^+$  and  $D^+$  no signal could be detected below 19.5 eV. Therefore the energy difference between measured and calculated onset has to be ascribed to the excitation of  $NH_2$  only, i.e.  $19.5 - 18.1 = 1.4$  eV. This energy difference is close to the excitation energy of  $NH_2$  in its  $^2A_1$  state found at 1.27 eV by optical spectroscopy (see table 2). The most probable mechanism to be invoked for the threshold at 19.5 eV is



and lies in the energy range of the  $NH_3^+(\tilde{A}^2E)$  state. From previous work, this state is known to be split by Jahn-Teller interaction into  $^2A' + ^2A''$  states [21] and to give rise to  $NH^+$  and  $NH_2^+$  by predissociation [21, 1]. The photoelectron band related to the  $\tilde{A}^2E$  state has a shape suggesting that this state is populated well above 16.9 eV [22], the lowest appearance energy of  $NH^+$  [1]. It seems to be likely that at 19.5 eV dissociative ionization is observed through the direct population of the  $\tilde{A}^2E$  ( $^2A' + ^2A''$ ) dissociation continuum. However, at the present time the fact that the lowest dissociation process calculated at 18.105 eV is not observed, remains unexplained.

The expected slope for the dissociation process involving  $H^+$  and  $NH_2$  is  $m_{NH_2}/m_{NH_3} = 16/17 = 0.94$ , while the observed slope is  $s = 0.49$ . This indicates that the excess energy with respect to the dissociation limit at 19.5 eV is shared to a large extent (about 50%) between translational and internal (essentially vibrational) energy of  $NH_2$ . This analysis is confirmed by the measurements on  $D^+/ND_3$ . A slope  $s_i = 0.29$  is observed instead of the expected value of  $m_{ND_2}/m_{ND_3} = 18/20 = 0.9$ .

Both processes involving vibrational energy content of  $NH_2$  and  $ND_2$ , the ratio of the two experimental slopes  $s_i/s$  has to be related to the isotope effect on the vibrational frequencies of both species. This isotope effect is usually measured by  $\rho = (v^1/v^2)^2$ . For a triatomic molecule of the type  $XY_2$ , the relationships between  $\rho$  and the

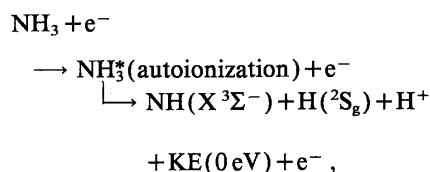
molecular masses are given by Herzberg [23]. When the antisymmetric frequency is chosen,  $\rho_3 = (v_3^1/v_3)^2=0.56$ , whereas for the symmetric vibrations  $\rho_{1,2}(v_{1,2}^1/v_{1,2})^2=0.28$ . A fairly good agreement is found between  $\rho_3$  and  $s_i/s=0.59$ , in spite of the poor correlator coefficient of the least-squares fit. This might be an indication that essentially  $v_3$  is active in this process.

As mentioned above, two investigations of dissociative excitation were performed on H atom formation from  $\text{NH}_3$ . Both studies include the kinetic energy distributions and threshold energy measurements. These results can be "extrapolated" to dissociative ionization work. Furthermore, Böse and Sroka [24] examined various H (Lyman) emissions produced by electron impact on  $\text{NH}_3$  without kinetic energy measurements.

Carnahan et al. [6] measured the first onset at  $17.8 \pm 0.8$  and  $23.2 \pm 0.7$  eV for H( $n=2$ ) and H (Rydb. ) atoms respectively. For both processes the minimum translational energy carried by the H atom is about 0.1 eV. Kurawaki and Ogawa [7] observed the first onset at  $21.0 \pm 0.8$  and  $22.5 \pm 0.8$  eV for H( $n=3$ ) and H( $n=4$ ) atoms carrying respectively 1.0 eV and 1.0 eV kinetic energy. None of these energies correlate with a dissociative ionization appearance energy of  $19.5 \pm 2$  eV. However, Böse and Sroka [ 24 ] measured an onset at  $16.1 \pm 0.4$  eV for H (Lym.- $\alpha$ ). When the energy difference of  $\text{IE}(\text{H}) - \text{EE}(\text{H}, n=2) = 3.4$  eV is added to this value, a threshold of  $19.5 \pm 0.4$  eV is obtained for  $\text{H}^+/\text{NH}_3$ .

In fig. 7 two onsets are observed around 22.6 eV, i.e.  $22.6 \pm 0.3$  eV, in the kinetic energy range 0-0.8 eV (see straight line (2) ), and  $22.4 \pm 0.1$  eV (see vertical line ( 3 ) ). This latter process is observed over the 2.8-4.3 eV kinetic energy range. Fig. 8 shows the result of the same measurements for  $\text{D}^+/\text{ND}_3$ .

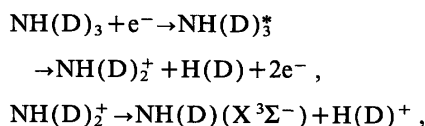
At  $22.6 \pm 0.3$  eV enough energy is available to produce the proton through



for which the lowest onset is calculated at  $22.01 \pm 0.2$  eV from the data listed in table 2. The higher excitation of  $\text{NH}_2$  although possible cannot be considered because of lack of data. If the energy difference of  $0.5 \pm 0.3$  eV in excess between experimental and calculated threshold is significant, it would be ascribed to internal energy of the NH radical, since no translational energy is available at the onset (see diagram (2) in fig. 7). From the following discussion, most likely, the excess energy above the onset is partitioned between vibrational and translational energy.

The straight line (2) starting at  $22.6 \pm 0.3$  eV is the result of a least-squares fit, has a slope of 0.89 and extrapolates to 22.51 eV. The correlation coefficient is rather poor, i.e. 0.93. The expected slope of  $\text{H}^+$ , produced through the abovementioned process, is roughly given by  $m_{\text{NH}}/2m_{\text{NH}_3} = 0.44$ . Notwithstanding the poor correlation, the discrepancy between experimental and expected slope is large. Furthermore, when the same fit is applied to the corresponding data of  $\text{D}^+/\text{ND}_3$  (see fig. 8, line (2) ), a straight line with a slope of 0.54 and extrapolating to 22.47 is obtained. The correlation is also 0.93. The slopes are significantly different: the eight onsets measured for  $\text{D}^+$  are systematically higher than the corresponding data for  $\text{H}^+$ . Moreover, as evidenced earlier in this discussion, for a diatomic radical  $\rho=(v^1/v)^2= \mu/\mu^1=0.94/1.75=0.54$ , whereas  $s_i/s \approx 0.5/0.9 \approx 0.55$ . These arguments tend to support a partition of the total excess energy between vibrational and translational energy.

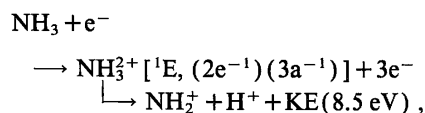
To account for the experimental results a two-step proton production mechanism has to be invoked, i.e.



where the proton carries  $15/16=0.94$  of the total translational energy, close to the observed slope. This agreement would suggest total energy conversion into translational energy. Expecting the same reaction sequence in  $\text{ND}_3$ , the theoretical slope for  $\text{D}^+$  would be 0.88 while the observed one is 0.54. This discrepancy can only be ascribed

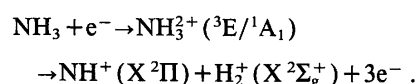




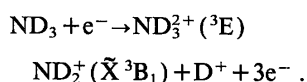


no onset is observed at this energy for  $\text{NH}_2^+$  nor  $\text{NH}^+$  [1]. An alternative explanation of this critical energy would be the dissociation of a highly excited, singly ionized  $\text{NH}_3^+$  state. In this case the  $\text{NH}_3^{2+}$  ionic state would be formed through autoionization which would compete with dissociation. Kurawaki and Ogawa [7] determined an excitation onset for  $\text{H}(n=4)$  atoms at  $38.4 \pm 1.5$  eV carrying 8-12 eV kinetic energy. Through the "core-ion" model, the corresponding dissociative ionization process would lie at about  $39.3 \pm 1.5$  eV accounting for  $\text{IE}(\text{H}) - \text{EE}(\text{H}, n=4) = 0.85$  eV. However, no  $\text{H}(\text{Rydb.})$  atoms have been detected in this energy range by Carnahan et al. [6].

Between 34.9 and 39.2 eV an onset at  $36.2 \pm 0.3$  eV is less clearly observed in the first differentiated ionization efficiency curve of  $\text{H}^+$ , but could be observed up to 4.3 eV kinetic energy. As it has already been pointed out [1], appearance energies were measured at  $36.6 \pm 0.3$  and  $36.2 \pm 0.4$  eV for  $\text{ND}_2^+/\text{ND}_3$  and  $\text{NH}^+/\text{NH}_3$ , respectively. It has been shown that the  $\text{NH}^+$  formation occurs through



The corresponding threshold for  $\text{ND}_2^+$  has been interpreted by

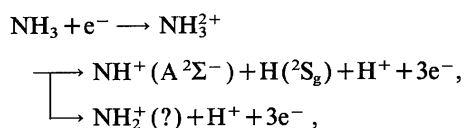


The onset for this process is calculated at 29.5 eV, using the data listed in table 2. The amount of total translational energy carried away by the fragments in this process would be 6.7 eV, i.e. 6 eV by  $\text{D}^+$  and 0.7 eV by  $\text{ND}_2^+$ . Experimentally  $\text{ND}_2^+$  is observed up to 0.9 eV whereas the  $\text{D}^+$  ion could be measured up to 4.3 eV kinetic energy.

As mentioned in section 3, the appearance energy at  $45.7 \pm 0.4$  eV could only be measured with a reasonable accuracy up to 1.0 eV kinetic energy. At this energy the  $\text{H}^+$  contribution very rapidly decreases with increasing retarding potential and the signal/noise ratio becomes worse.

For  $\text{ND}_2^+$  as well as  $\text{NH}^+$  a threshold energy is measured at  $46.5 \pm 0.4$  and  $46.4 \pm 0.5$  eV; the ions carrying at least 0.7 and 0.9 eV translational energy respectively [1]. Probably these critical energies are related to one another. In addition PIPICO measurements were performed in this energy range and a component, unresolved with respect to  $m/e=14$  and  $m/e=15$ , has an onset at  $44.5 \pm 0.5$  eV. On the other hand,  $\text{H}(n=4)$  [7]  $\text{H}(\text{Rydb.})$  atoms [6] were observed up to  $41.7 \pm 1.7$  eV with translational energies of 8-12 eV.

At this energy, the proton is very likely produced through both



even when for experimental reasons  $\text{H}^+$  ( $\text{D}^+$ ) could not be observed at  $V_R > 1.0$  V. On the basis of the data listed in table 2 and the observed 7.6 eV total translational energy carried by  $\text{NH}^+$  [1], the energy required for the abovementioned  $\text{NH}^+$ -producing process is 45.8 eV.

In the  $\text{NH}_2^+$  dissociation channel, the measurements were performed on  $\text{ND}_3$ . On  $\text{ND}_2^+$  only 0.7 eV kinetic energy is measured, i.e. 7 eV total translational energy. The  $\text{D}^+$  ion is observed up to 1 eV kinetic energy. The highest dissociation limit for  $\text{ND}_2^+$  formation, which could be calculated from the data listed in table 2, lies at 32.7 eV. By adding 7 eV total translational energy of the fragments, an energy of 39.7 eV is obtained. The energy difference of about 7 eV between the observed onset and the foregoing energy balance could only be

ascribed to the excitation of  $\text{ND}_2^+$ .

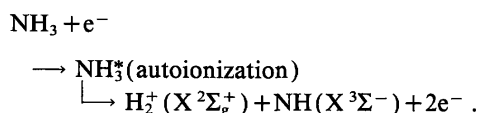
#### 4.2. The $\text{H}_2^+$ ( $\text{D}_2^+$ ) dissociation channel

The lowest appearance energy measured for both  $\text{H}_2^+$  and  $\text{D}_2^+$  (see figs. 10 and 11) lies at  $15.5 \pm 0.2$  eV. This value is in very good agreement with that published by Mann et al. [2], who observed only one onset at  $15.5 \pm 0.5$  eV. Mark et al. [3] mentioned a threshold at  $14.8 \pm 0.2$  eV.

At this energy the first differentiated ionization efficiency curve rises very steeply and this part of the curve is suppressed by applying 0.2 V retarding potential. The  $\text{H}_2^+$  ( $\text{D}_2^+$ ) ions produced at 15.5 eV are thermal and are the only contribution to the thermal peak observed in the kinetic energy distribution displayed in fig. 9. Moreover, the ionization energy of molecular  $\text{H}_2$  is 15.496 eV (see table 2), in very good agreement with the onset energy for  $\text{H}_2^+$  ( $\text{D}_2^+$ ) in this work. Together these arguments strongly suggest that free  $\text{H}_2$  is produced from  $\text{NH}_3$  in the ion source (likely by thermolysis on the electron emitting filament). The same phenomenon is observed for  $\text{ND}_3$ .

The first onset ascribed to  $\text{H}_2^+$  ( $\text{D}_2^+$ ) formation through dissociative ionization of  $\text{NH}_3$  ( $\text{ND}_3$ ) lies at  $22.3 \pm 0.2$  eV. Its dependence upon the retarding potential is given by a vertical line (1) in fig. 12. Within experimental error, the data related to  $\text{H}_2^+$  and  $\text{D}_2^+$  behave in the same way.

The lowest threshold which could be calculated for  $\text{H}_2^+$  production from  $\text{NH}_3$  is at  $19.45 \pm 0.18$  eV by using the data listed in table 2. This energy corresponds to the reaction



Experimentally both  $\text{H}_2^+$  and  $\text{D}_2^+$  carry away 3.4 eV kinetic energy. The appearance energy  $\text{AE}(\text{H}_2^+)_{\text{KE}=0} = 22.3 - 3.4 \times 17/15 = 18.5$  eV. This value is lower than that for the predicted dissociation mechanism mentioned above. The discrepancy between calculated onset and latter value is about  $1.0 \pm 0.4$  eV. In the discussion of the results on the  $\text{NH}_2^+$  and  $\text{NH}^+$  ion formation [1], discrepancies of  $0.24 \pm 0.13$  and  $0.5 \pm 0.3$  eV have already been mentioned. They were ascribed to an overestimate of one or both dissociation energies  $D$  ( $\text{NH}_2\text{-H}$ ) and ( $\text{NH-H}$ ).

Considering all the fragment ions studied so far, appearance energies are measured at about 22.6 eV for  $\text{NH}_2^+$  [1],  $\text{NH}^+$  [1],  $\text{H}^+$  (see table 1) and  $\text{H}_2^+$ . This critical energy lies where no ionization cross section is measured for  $\text{NH}_3$  [25]. All abovementioned ions are formed with large amounts of kinetic energy. The neutral  $\text{NH}_3^*$  state is very likely a Rydberg state, member of a series converging to the  $\text{NH}_3^+$  ( $\tilde{\text{B}}^2\text{A}_1$ ) state. This latter being almost dissociative, the  $\text{NH}_3^*$  state is very probably unstable in all the dissociation channels. Therefore dissociative autoionization will be the most probable mechanism of  $\text{H}_2^+$  formation at 22.3 eV.

From  $26.6 \pm 0.3$  eV the first derivative of the ionization efficiency curve of  $\text{H}_2^+$  ( $\text{D}_2^+$ ) rises more steeply. The kinetic energy versus appearance energy plot is shown in fig. 12 by diagram (2). Owing to the scattering of the measurements, the data related to  $\text{H}_2^+$  and  $\text{D}_2^+$  are not distinguishable. From 0.2 eV translational energy, the data more or less clearly deviate from a vertical line at about 26.6 eV.

Taking into account all the measurements related to both  $\text{H}_2^+$  and  $\text{D}_2^+$ , the best correlation is found when gathering the data into two groups. Two fits are found by this way: (i) a first straight line between 0.2 and 1.4 eV kinetic energy, with a slope of 0.9 extrapolating to 26 eV with a correlation of 0.8 and (ii) a second straight line spread over 1.4-2.0 eV with a slope of 0.35 extrapolating to 23.0 eV with a correlation coefficient of 0.95.

The slope expected for the kinetic energy versus appearance energy straight line depends on the dissociation mechanism involved,



ion current, formed at 22.6 eV, is produced by the spontaneous dissociation of  $\text{NH}_2^+$ . The same mechanism is invoked for a part of the  $\text{H}_2^+$  ion current observed at 26.2 eV. The  $\text{H}^+$  ions appearing at this latter energy could be produced by dissociative ionization of  $\text{H}_2$ .

In the high electron energy range of 35-50 eV, mainly direct dissociation of doubly ionized states of  $\text{NH}_3$  is involved. Most of the processes invoked to account for the experimental data have already been discussed for the appearance of  $\text{NH}_2^+$  and  $\text{NH}^+$  from  $\text{NH}_3$  in a previous work [1]. Though a double ionization energy of  $\text{NH}_3$  was measured at 39.5 eV and an  $\text{H}^+$  formation threshold at about the same energy, very likely a dissociation of a highly excited, singly ionized  $\text{NH}_3$  state is involved.

### **Acknowledgement**

We acknowledge the Fonds de la Recherche Fondamentale Collective (FRFC), the Université de Liège and the Action de Recherches Concertées (ARC) of the Belgian Government for financial support. One of us (ML) wishes to thank the Belgian Government for a PREST grant.

### **References**

- [1] R. Locht, Ch. Servais, M. Ligot, F. Derwa and J. Momigny, *Chem. Phys.* 123 (1988) 443.
- [2] M.M. Mann, A. Hustrulid and J.T. Tate, *Phys. Rev.* 58 (1940) 340.
- [3] T.D. Mark, F. Egger and M. Cheret, *J. Chem. Phys.* 67 (1977) 3795.
- [4] G.R. Wight, M.J. van der Wiel and C.E. Brion, *J. Phys. B* 10 (1977) 1863.
- [5] C.E. Brion, A. Hamnett, G.R. Wight and M.J. van der Wiel, *J. Electron Spectry.* 12 (1977) 323.
- [6] B.L. Carnahan, W.W. Kao and E.C. Zipf, *J. Chem. Phys.* 74 (1981) 5149.
- [7] J. Kurawaki and T. Ogawa, *Chem. Phys.* 86 (1984) 295.
- [8] K.C. Smyth, J.A. Schiavone and R.S. Freund, *J. Chem. Phys.* 59 (1973) 5225.
- [9] R. Locht, J.L. Olivier and J. Momigny, *Chem. Phys.* 43 (1979) 425; 49 (1980) 173.
- [10] R. Locht and J. Momigny, *Chem. Phys. Letters* 138 (1987) 391.
- [11] R. Locht and J. Schopman, *Intern. J. Mass Spectrom. Ion Phys.* 15 (1974) 361.
- [12] Ch. Servais, R. Locht and J. Momigny, *Intern. J. Mass Spectrom. Ion Processes* 71 (1986) 179.
- [13] K. Köllman, *J. Phys. B* 11 (1978) 339.
- [14] B. de B. Darwent, *Bond dissociation energies in simple molecules*, NSRDS NBS 31 (1970).
- [15] G. Herzberg, *Molecular spectra and molecular structure*, Vol. 1. *Spectra of diatomic molecules* (Van Nostrand, Princeton, 1950).
- [16] S.J. Dunlavey, J.M. Dyke, N. Jonathan and A. Morris, *Mol. Phys.* 39 (1980) 1121.
- [17] C.E. Moore, *Atomic energy levels*, Vol. 1, NBS Circ. 467 (1949).
- [18] G. Herzberg, *Molecular spectra and molecular structure*, Vol. 3. *Electronic spectra and electronic structure of polyatomic molecules* (Van Nostrand, Princeton, 1967).
- [19] K.P. Huber and G. Herzberg, *Molecular spectra and molecular structure*, Vol. 4. *Constants of diatomic molecules* (Van Nostrand, Princeton, 1979).
- [20] R. Colin and A.E. Douglas, *Can. J. Phys.* 46 (1968) 61.
- [21] C. Krier, M.Th. Praet and J.C. Lorquet, *J. Chem. Phys.* 82 (1985) 4073.
- [22] J.W. Rabalais, L. Karlsson, L.O. Werme, T. Bergmark and K. Siegbahn, *J. Chem. Phys.* 58 (1973) 3370.



*Published in: Chemical Physics (1988), vol. 125, pp. 425-437.*  
*Status: Postprint (Author's Version)*

[23] G. Herzberg, *Molecular spectra and molecular structure*, Vol. 2. *Infrared and Raman spectra of polyatomic molecules* (Van Nostrand, Princeton, 1945).

[24] N. Böse and W. Sroka, *Z. Naturforsch.* 26a ( 1971 ) 1491.

[25] G. Bieri, L. Åsbrink and W. von Niessen, *J. Electron Spec-try.* 27 (1982) 129.

[26] D. Winkoun and G. Dujardin, *Z. Physik D* 4 (1986) 57.